International Journal of Fluid Machinery and Systems
Vol. 3, No. 1, January-March 2010

Original Paper

Cavitation Surge Suppression of Pump Inducer with Axi-asymmetrical Inlet Plate

Jun-Ho Kim[4], Koichi Ishzaka[2], Satoshi Watanabe[1] and Akinori Furukawa[3]

[1]Department of Mechanical Engineering, Kyushu University
740 Motooka Nishi-ku, Fukuoka, 819-0395, Japan, fmnabe@mech.kyushu-u.ac.jp,
[2]ishizk@mech.kyushu-u.ac.jp, [3]fmfuru@mech.kyushu-u.ac.jp
[4]Hyosung Ebara Co. Ltd.,
43-1 Ungnam-Dong, Changwon-Si, 641-290, Korea, hec-kjh@hyosung.com

Abstract

The attachment of inducer in front of main impeller is a powerful method to improve cavitation performance. Cavitation surge oscillation, however, often occurs at partial flow rate and extremely low suction pressure. As the cavitation surge oscillation with low frequency of about 10 Hz occurs in a close relation between the inlet backflow cavitation and the growth of blade cavity into the throat section of blade passage, one method of installing an axi-asymmetrical plate upstream of inducer has been proposed to suppress the oscillation. The inlet flow distortion due to the axi-asymmetrical plate makes different elongations of cavities on all blades, which prevent the flow from becoming simultaneously unstable at all throat sections. In the present study, changes of the suppression effects with the axial distance between the inducer inlet and the plate and the changes with the blockage ratios of plate area to the cross-sectional area of inducer inlet are investigated for helical inducers with tip blade angles of 8° and 14°. Then a conceivable application will be proposed to suppress the cavitation surge oscillation by installing axi-asymmetrical inlet plate.

Keywords: Turbomachinery, Pump inducer, Cavitation surge suppression, Axi-asymmetrical inlet plate

1. Introduction

Recently, the miniaturization of turbopumps has been expected to reduce the pump space for various hydraulic systems. Though high-speed operation is necessary for this purpose, it might lead to the occurrence of cavitaion, then the deterioration of cavitation performance of turbopumps. The attachment of an inducer upstream of a main impeller is a powerful method to achieve the high cavitation performance in severe suction pressure conditions [1][2]. However, the various cavitaion instabilities are known to occur even at designed flow rate as well as in the partial flow rate range, causing severe shaft vibrations and strong flow fluctuations [3][4][5]. The low cycle cavitation surge oscillation, focused in the present paper, is a viciously unstable phenomenon occurring at partial flow rates, in which all blade cavities in the inducer become periodically and synchronously elongated and shortened and the flow rate fluctuates. The operation under the occurrence of cavitation surge is considered to be very dangerous, because the low frequency of the cavitation induced oscillation possibly coincides with the resonance of pump system. Therefore the development of methods to avoid and control the cavitation surge phenomenon is expected in the realization of safety operation in wide flow rate range of downsized and high-speed turbopump. There have been some trials to control cavitation instability phenomena passively, as Kamijo's method [6] to avoid the rotating cavitation by the suction pipe with weak contraction at the inducer inlet, Kurokawa's method [7] to control a rotating backflow cavitation by an adoption of J-groove, i.e., many grooves on the casing at the inlet, and authors' method [8] to suppress the backflow cavitation occurring at the inducer inlet tip by installation of a ring-shaped axi-symmetric inlet plate, which blocks the backflow appearing from the blade tip region of the inducer.

On the other hand, authors [9] have clarified that the cavitation surge oscillation occurred when the tail ends of all cavities on the blades were simultaneously elongated into the inlet throat sections of blade passages. This report demonstrates that an axi-asymmetry inflow might be effective to control of cavitation induced oscillation. Then, it was confirmed by experiments with one

Received November 16 2009; accepted for publication December 10 2009: Review conducted by Prof. Zhang Yang-jun. (Paper number O09050)
Corresponding author: Akinori Furukawa, Professor, fmfuru@mech.kyushu-u.ac.jp

inducer of tip blade angle 14° [10] that cavitation surge oscillation can be suppressed by the installation of obstacle plate, which is axi-asymmetry type, upstream of inducer. In the present study, the effects of the distance between the obstacle plate and inducer inlet and the blockage ratio of the area of obstacle plate to flow passage area on cavitation surge suppression are investigated for two kinds of flat-plate helical inducers with different blade angle. In addition, the practical use of this method is proposed with installation of a sluice valve upstream of inducer inlet.

2. Experimental Apparatus

Experiment has been done with a closed loop cavitation tunnel [10]. Figure 1 shows a schematic view of test section. Two kinds of inducers were tested, which are flat plate helical type with blade number of 2, tip solidity of 2.0, blade tip diameter of D=64mm, hub-tip ratio of 0.47. Blade tip angle of each inducer is β_{1t} =8° or 14°, respectively. The tip clearance between blade tip and suction casing surface is 0.5mm. Figure 2 shows three kinds of axi-asymmetric type obstacle plates, the blockage ratios of which to cross-sectional area of flow passage are changed to 26.5%, 49.5% and 69.4%. Each obstacle is denoted as [BP027], [BP050] or [BP069], respectively. These obstacles are installed at the upstream section of L/D=0.177 to 0.789 from the inducer leading edge, by replacing the axial position of inducer relatively to the stationary obstacle plate as depicted in Fig.1, where L means the distance between the obstacle plate and inducer inlet.

Cavitation tests were performed after pre-operation under cavitating conditions of low NPSH for a long time for the purpose of deaeration. The rotational speed was kept constant as N=5000min^{-1} with the deviation of 0.1%. The mean flow rate Q was measured by a turbine-type flow meter with the error less than 2%. The inducer head H was evaluated from the wall pressure difference between the sections ① and ② in Fig.1 with taking account of guide-vane losses up- and downstream of the inducer and the change of dynamic head. The NPSH ($=H_{sv}$) was calculated from the total head at the section ① with taking account of guide-vane loss upstream of inducer and water temperature. In this experiment, the additional loss of installing the obstacle is included in evaluating the inducer head H, taking lower value due to the obstacle loss, and the NPSH, from considering that the pump NPSH should be evaluated as total system of a combination of obstacle and inducer though the value of NPSH at the inducer inlet is also dropped by the obstacle loss. The cavitation experiments were carried out with decreasing dimensionless NPSH $\tau=gH_{sv}/U_t^2$, where g is gravitational acceleration, under the condition of the constant flow coefficient ϕ, defined as $\phi=Q/AU_t$, where A is cross-sectional area of the flow passage and U_t is inducer tip speed. The measurement of static pressure fluctuations on the casing wall and the visual observation of the cavities with a high speed video camera with 1000frame/sec were made to understand the flow structure as well as to judge the occurrence of cavitaiton surge.

3. Results and Discussions

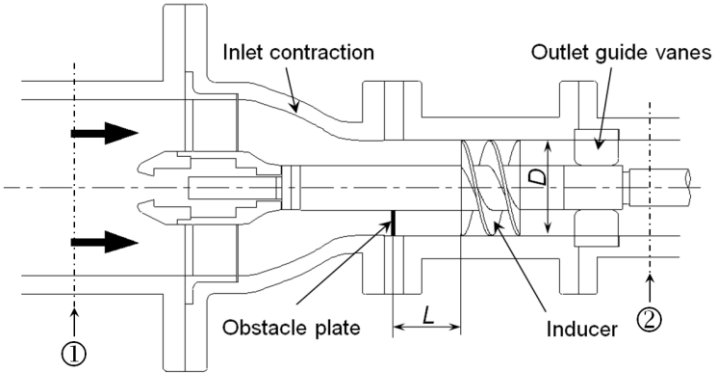

Fig. 1 The sectional view of test pump

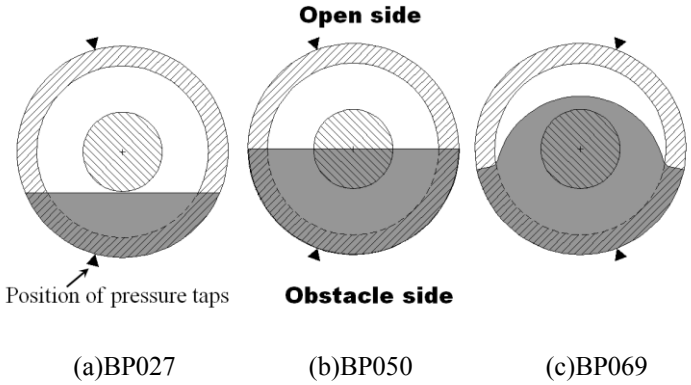

Fig. 2 Axi-asymmetrical obstacle plates

3.1 Effects of Obstacle Plate Blockage Ratios

Effects of obstacle blockage ratios on inducer performance and cavitation surge oscillation were, at first, investigated under the condition of constant distance of L/D=0.555 between the obstacle and inducer inlet. Figure 3 shows the head-rise characteristics of the test inducers with/without the obstacle plates at the sufficiently high NPSH without the occurrence of the cavitation. The abscissa denotes the flow coefficient ϕ and the ordinate of the upper figure denotes the head-rise coefficient of $\psi=H/(U_t^2/g)$. The lower figure shows the additional flow loss coefficient of $\psi_{loss}=H_{loss}/(U_t^2/g)$ due to installation of each obstacle plate. Seeing results of β_{1t} =14° inducer, its head is deteriorated over all flow rate range by installing the obstacle plates but the amount of deterioration dose not directly correspond to the additional loss ψ_{loss}. The deterioration of inducer head is larger than the amount of additional loss in partial flow rate range of ϕ<0.07, where the backflow appears in the tip region of inducer inlet, but becomes smaller in over flow rate range. This result demonstrates that non-uniform flow due to installing the obstacle plate yields the change of inducer head rise mechanism itself in the inducer flow passage. It means that the accurate prediction of head deterioration due to the installation might be required in the case of installing the obstacle at all times in the practical use because

the role of inducer is to increase the inlet pressure of main impeller. Seeing results of β_{1t} =8° next, the amount of head deterioration due to installing the obstacle becomes smaller than that of β_{1t} =14° inducer since the flow rate range of positive head appearance (ψ>0) moves to lower side than the case of β_{1t} =14° inducer. But, the tendency of inducer head deterioration is almost the same as that of β_{1t} =14° inducer.

Figure 4 shows the cavitation performance curves of the inducer without/with the axi-asymmetric obstacle plates at m =0.07, where the flow rate ratio m is denoted as $m=\phi/\tan\beta_{1t}$ that is the flow coefficient ϕ normalized by the shockless flow rate $\tan\beta_{1t}$. The operating points under cavitation surge oscillation are depicted as solid symbols. In the case without the obstacle plate as the

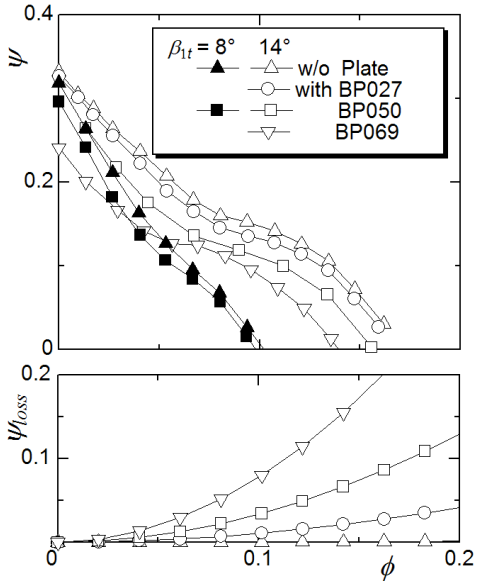

Fig. 3 Inducer head characteristics at high NPSH and head loss of obstacle plates

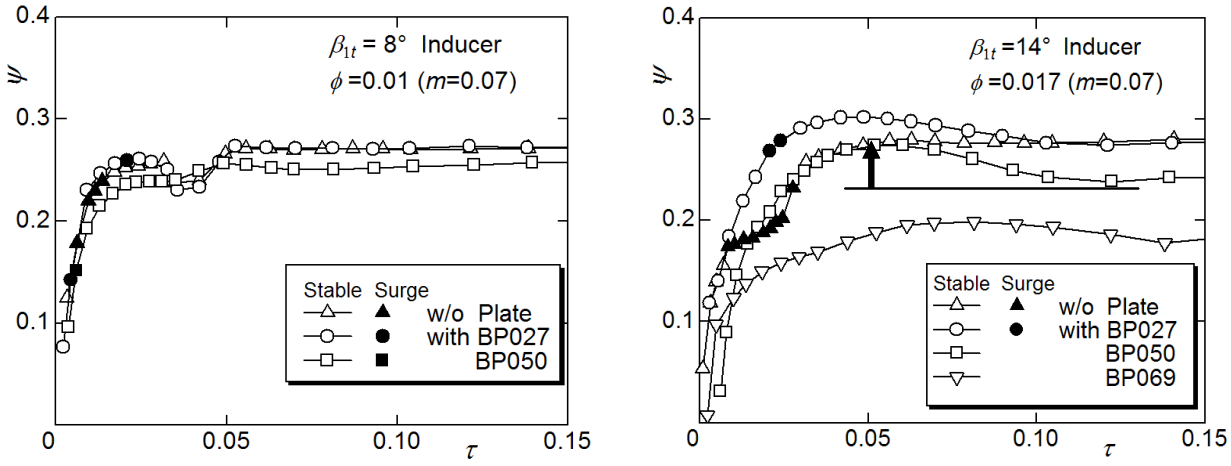

(a) β_{1t}=8° inducer at ϕ=0.01 (m =0.07) (b) β_{1t}=14° inducer at ϕ=0.017 (m =0.07)

Fig. 4 Change of cavitation performance with obstacle plates

symbol of △ and ▲ in Fig.4, it can be seen that the cavitation surge oscillation is observed with deep head deterioration in the region of ▲ in Fig.4, irrelevant to inducer blade angles. In Fig.4(a) of β_{1t} =8° inducer, cavitation surge oscillation is almost suppressed by installing the obstacle, except for at two points of τ=0.025 and 0.007 (● in Fig.4(a)) in the case of [BP027] and at one point of τ=0.01 (■ in Fig.4(a)) in the case of [BP050], where cavitation surge oscillation still occurs. In Fig.4(b) of β_{1t} =14° inducer, the oscillation is also suppressed by installing obstacle except for only at the point near τ=0.025 in the case of [BP027]. In cases of [BP050] and [BP069] the oscillation is completely suppressed. When the axi-asymmetrical obstacle plate is installed upstream of β_{1t} =14° inducer, the following phenomena appears on the cavitation performance curves. At higher NPSH of τ>0.15 the inducer head becomes lower with increase of the blockage ratio of obstacle due to the additional head loss. On the other hand, the inducer head is conversely increased with decrease of NPSH at the condition just before head breakdown. The range of NPSH where head is increased doesn't seem to be similar with each obstacle with different blockage ratio and the head increment of

[BP050] is the largest among three obstacles as seen as an arrow in Fig.4(b).

Figure 5 shows static head rise $\Delta\psi$ on the casing wall at upstream section of inducer inlet in the case of β_{1t} =14° inducer. $\Delta\psi$ ($=\Delta h/(U_t^2/g)$, Δh: static head difference) is denoted as the dimensionless static head difference between the section upstream of inducer inlet by 8mm and the section ① in Fig.1. Two taps on the wall at the same axial position were installed to measure static head simultaneously in both sides with/without obstacle, the circumferential positions of which are depicted as the symbol of ▲ in Fig.2. In the case of installing obstacle, static head in the side without obstacle (Open side in Fig.2) is higher than that in the side with obstacle (Obstacle side in Fig.2). Among various static head curves in Fig.5, the static head increment in open side of [BP050] takes the largest as the symbol of □, that is the same tendency of inducer head in Fig.4. This cause is considered as follows. The through-flow in each flow passage of two-bladed inducer becomes different due to inlet flow distortion due to the axi-asymmetric obstacle. This non-uniformity is increased by the difference of backflow size and the cavity volume at the tip region of inducer inlet. As the result, one of the two blades has so high loading, yielding the higher head, then the static head in one of the backflow regions becomes also increased. This phenomenon will be clarified by further measurement of wall pressure and velocity distribution in our future work. On the other hand, the behavior of such static head rise in low NPSH region as β_{1t}=14° inducer in Fig.4(b) did not recognized in the case of β_{1t}=8° inducer as seen in Fig.4(a).

Figure 6 summarizes the onset region of the cavitation surge oscillation for various flow rates. The onset regions are determined from the results of the frequency analysis of the wall pressure fluctuations upstream and downstream of inducer and the visual observation of cavity oscillation with the high-speed video camera. The abscissa and ordinate denote the flow rate ratio m and the normalized NPSH ($=\tau/\tan^2\beta_{1t}$), respectively. The cavitation surge occurs in the range (band) of τ between two lines with constant m or at the unique operating point of ○ or △ shown for each case. In the case without the obstacle plate, the onset region of cavitation surge in β_{1t}=8° inducer (thin broken lines) clearly becomes wider than that of β_{1t}=14° inducer (thin solid lines). On the other hand in the case of installing the obstacle [BP027], the the onset surge region in β_{1t}=8° inducer (thick broken lines) becomes further wider and the appreciable suppression is not observed in large flow rate region as the range is moved to higher NPSH range though the band of the cavitation surge occurring range of τ becomes a little narrower in large flow rates range. However, the cavitation surge oscillation is completely suppressed in small flow rate range of m<0.1 in the case of [BP027] and as seen in Fig.6, the range becomes extremely narrow at about m=0.2 though the reason is not found at the present stage. In the case of [BP050] the cavitation surge oscillation of β_{1t}=8° inducer occurs only in narrow range of NPSH as the symbol of ○ in Fig.6 and the sufficient effect of suppression is found in other regions of NPSH and flow rate. Seeing results of β_{1t}=14° inducer, there is no appearance of cavitation surge onset region in the case of [BP050] and [BP069] as the same tendency as that of β_{1t}=8° inducer. It is found from Fig.6 that the appearance of suppression effect of cavitation surge depends on the inducer blade angle and the blockage ratio of the obstacle. As the reason of this difference, the changes of three-dimensional structure of backflow at the tip region of inducer inlet and the flow behavior at the inlet throat section with inducer blade angle are considered. This consideration will be also discussed after further measurement of inlet flow of each inducer in our future work.

3.2 Effects of Axial Distance between Position of Obstacle Plate and Inducer Inlet

Effects of axial distance between the position of obstacle plate and inducer inlet on inducer performance and cavitation surge

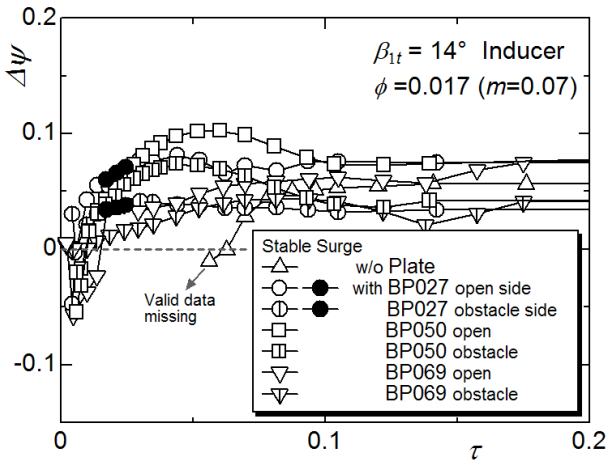

Fig. 5 Static head difference at obstacle side and open side of β_{1t}=14° inducer inlet at ϕ=0.017

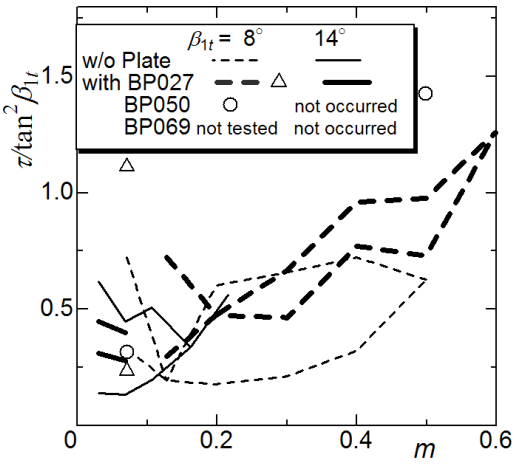

Fig. 6 Change of occurrence region of cavitation surge oscillation with cross sectional blockage ratio of obstacle plate

oscillation were, next, investigated under the condition of constant blockage ratio of obstacle plate [BP027]. The axial distance was changed in L/D=0.177 to 0.789. Figure 7 shows cavitation performance curves of β_{1t}=8° inducer in the case of [BP027] with various L/D at m=0.07. As can be surmised from Fig.7, head-rise characteristics in no-cavitation condition and cavitation performance curve in higher region of NPSH are not significantly changed with L/D.

Figure 8 summarizes the change of onset region of the cavitation surge oscillation with the installing position of obstacle plate for various flow coefficients. In the case of β_{1t}=14° inducer in Fig.8(a), the flow rate and NPSH ranges of cavitation surge occurring become wider, as found from double dotted lines in Fig.8(a), as the axial distance is increased from L/D=0.555 to 0.789 and the range is approached to that of the case without obstacle as the broken line in Fig.8(a). This means that the flow distortion due to the obstacle plate becomes weakened through the flow in the downstream direction to inducer inlet so that the effect of non-uniform elongation of blade cavity on each blade would disappear. When the distance is conversely shortened from L/D=0.555 the range becomes narrower and only the appearance of cavitation surge oscillation is limited in flow rate range near shut off one. But in the case of shortened L/D the range of NPSH of the cavitation surge occurring is wider and the cavitation surge occurs at higher NPSH as a single dotted line in Fig.8(a).

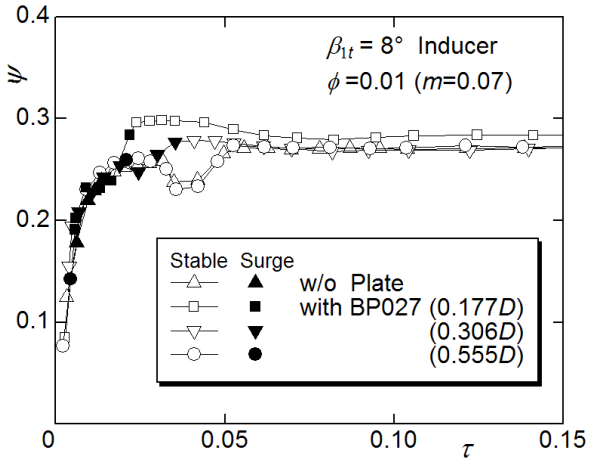

Fig. 7 Change of cavitation performance with distance L/D for β_{1t}=8° inducer with BP027 at ϕ=0.01

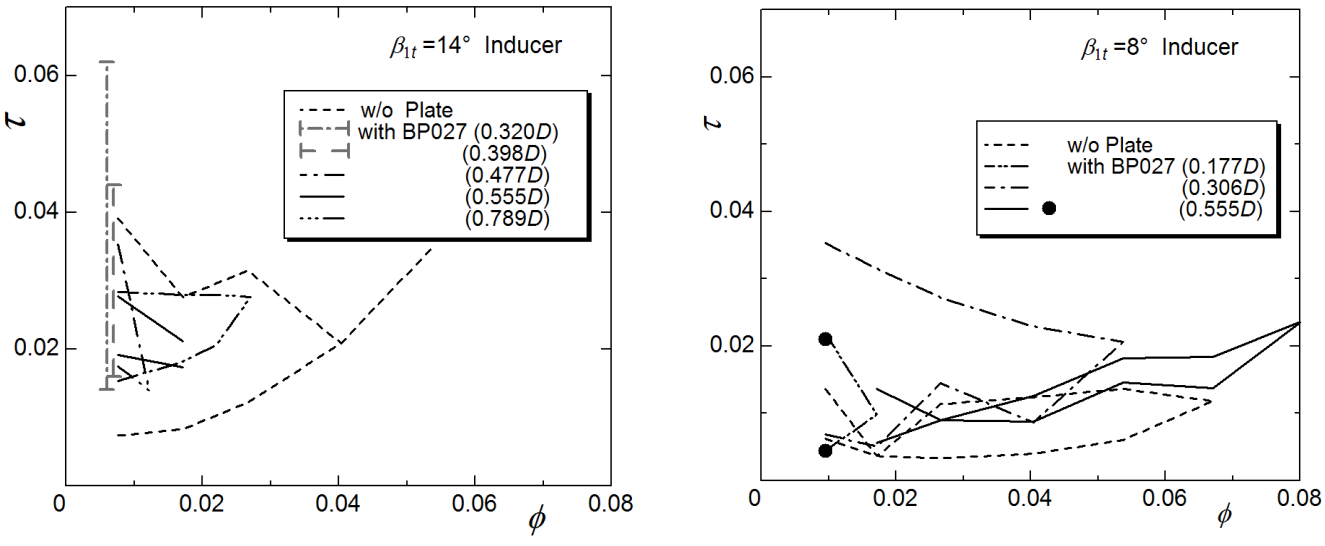

(a) β_{1t}=14° inducer (b) β_{1t}=8° inducer

Fig. 8 Change of occurrence region of cavitation surge oscillation with distance L/D of obstacle plate

Figure 9 shows comparisons of photos of cavitation behaviors in β_{1t}=14° inducer at ϕ=0.008 and τ= about 0.049. Figures 9(a) to (d) correspond to the cases of no obstacle, L/D=0.398, 0.555 and 0.789 in order, where the cavitation surge starts occurring at τ=0.04, 0.044, 0.028 and 0.03, respectively. The cavitation behaviors near the obstacle plate cannot be observed due to the restriction of apparatus. The circumferential position of axi-asymmetric obstacle plate is shown in the bottom of each photo in

Fig.9. As these behaviors in Fig.9 were taken in one circumferential direction, the difference of cavitation behavior due to circumferential position such as open and obstacle sides as shown in Fig.2 is not discussed directly from Fig.9. However the following results are obtained from the observation of cavitation behavior with synchronized stroboscopic-light. The obvious difference between the cavity lengths of open and obstacle sides is found in the case of L/D=0.555. On the other hand in the cases of L/D=0.398 (the shortened distance) and 0.789 (the elongated distance), the difference of cavity lengths in both sides is not cleared and the behaviors in these cases are almost similar to that in the case of no obstacle.

The change of onset region of the cavitation surge oscillation with the installing position of obstacle plate in the case of β_{1t}=8° inducer is shown in Fig.8(b). When the distance is shortened to L/D=0.306, the flow rate range where the suppression appears becomes narrower as a dotted line in Fig.8(b) but the NPSH range is wider and the onset appears at higher NPSH than the case of no obstacle. When the distance is further shortened to L/D=0.177, the flow rate and the NPSH ranges of cavitation surge occurring become narrower and the suppression effect clearly appears as a double dotted line in Fig.8(b). It is found from Figs.6 and 8 that the axi-asymmetrical plate with larger blockage ratio of flow passage should be installed at shorter distance from the inducer inlet to suppress the cavitation surge oscillation as the blade angle of inducer becomes smaller.

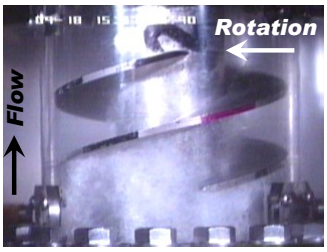

(a) without obstacle at τ=0.049

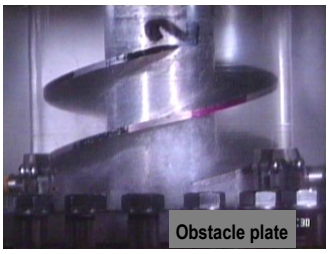

(b) with BP027, L/D=0.398 at τ=0.050

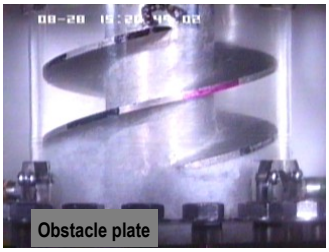

(c) with BP027, L/D=0.555 at τ=0.049

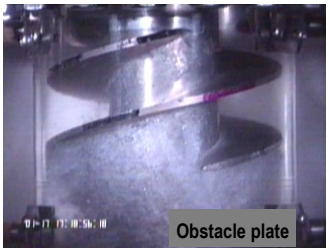

(d) with BP027, L/D=0.789 at τ=0.047

Fig. 9 Change of cavitation behavior with distance L/D of obstacle plate in β_{1t}=14° inducer at ϕ=0.008

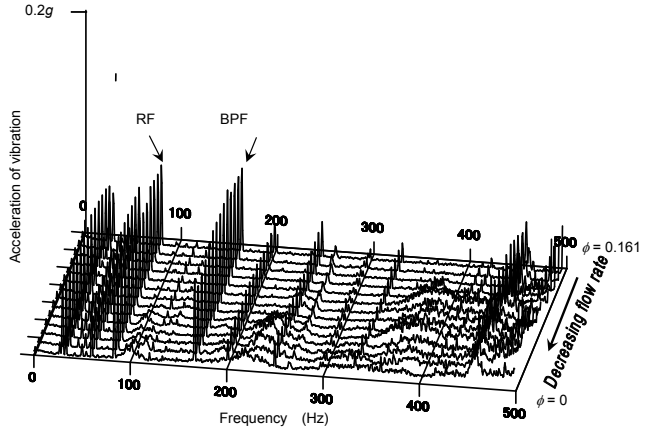

(a) No obstacle plate

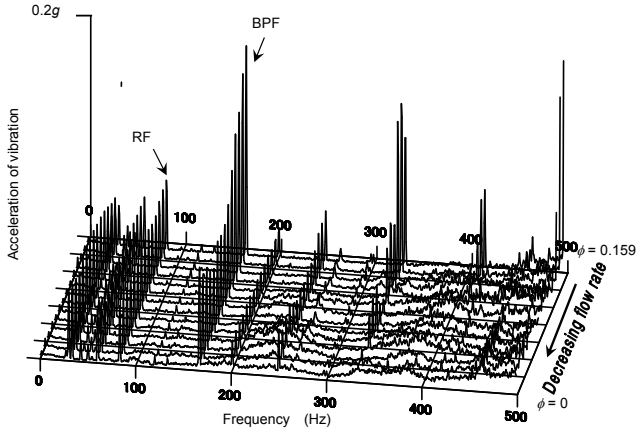

(b) Obstacle [BP027] at L/D=0.555

Fig. 10 Spectrum of measured vibration on test apparatus during head characteristics test of β_{1t}=14° inducer

3.3 Application of Axi-asymmetrical Obstacle Plate Installed Upstream of Inducer to Practical Use

It is clarified in previous section that an installation of axi-asymmetrical obstacle plate, when the blockage ratio of flow passage area and its installing position upstream of the inducer are appropriately selected, enables to suppress the cavitation surge occurring. However the way of installing the obstacle plate at all times to flow passage area yields decreasing the inlet pressure at the main impeller inlet due to the additional loss of the installation, which is similar with the case of the axi-symmetrical ring-

plate installation for suppression of cavitation surge [8]. This decrease of inlet pressure weakens the improvement of cavitation performance of the pump by inducer. In addition, the installation of fixed obstacle plate at all times gives the flow distortion at the inducer inlet, which causes the increasing of pressure fluctuation and vibration with rotational frequency of shaft (RF) and blade passing frequency (BPF). Figure 10 shows the result of frequency analysis of measured vibrations by the accelerometer that installed on the outer surface of discharge pipe downstream of inducer at high NPSH, where head characteristics as Fig.2 is obtained. It is found from Fig.10(b) that the amplitude of BPF and its harmonics become increased by installing the axi-asymmetrical obstacle plate even at ϕ=0.144 near the designed flow coefficient. On the other hand in partial flow rate range near the shut off, where cavitation surge oscillation appears, the increase of amplitude of vibration due to the installing the obstacle is not so large. Therefore, to avoid this vibration problem due to installing the obstacle at all times, we recommend the sluice-valve type of obstacle as shown schematically in Fig.11. The sluice-valve type of obstacle is installed at the appropriate distance upstream of inducer. By combination of a method on advance detection of cavitation surge oscillation [11], the sluice-gate is inserted by appropriate blockage of flow passage area when the pre-cursor of cavitation surge oscillation is detected. By this combination, the insert of obstacle plate is restricted to use in low NPSH and partial flow rate ranges, where the inducer head is sufficient for improving the cavitation performance of the pump. As the result, the vibration problem due to the installation of axi-asymmetrical obstacle at all times can be avoided.

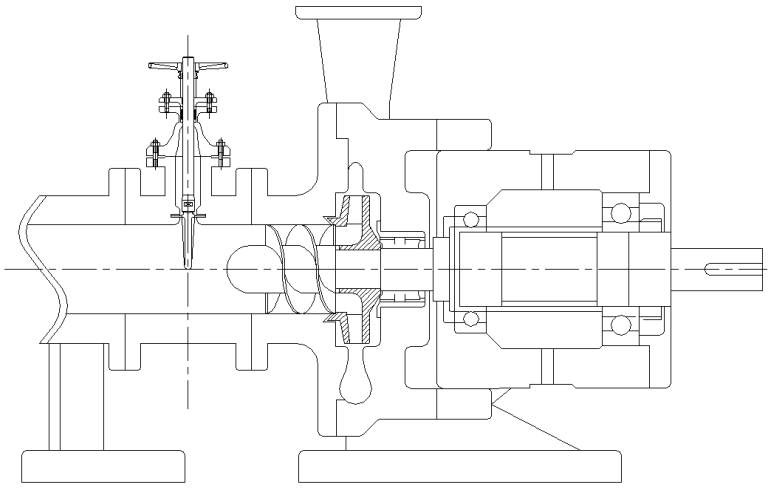

Fig. 11 Conceptual installation view of obstacle plate at pump section

4. Conclusions

Related on installing an axi-asymmetrical obstacle plate upstream of inducer inlet, which is effective to suppress the cavitation surge oscillation, experimental tests with various axial positions of the obstacle to inducer inlet and various blockage ratios against flow passage area have carried out for two kinds of inducers with β_{1t}=8° and 14° in order to investigate inducer performance and cavitation surge suppression effects. Results to obtain the suppression effect in wider operation range are summarized as follows:

1) As the appropriate blockage ratio of the obstacle against the flow passage area, the blockage of about 50% is recommended.
2) As the appropriate position of the obstacle installation, the axial distance upstream of inducer inlet should be selected in response to blade angle of inducer. The distance is shorter as the blade angle is smaller.
3) The installation of axi-asymmetrical obstacle at all times might cause a vibration problem even in normal operation condition at high NPSH. The suppression becomes so effective at partial flow rate and low NPSH that the sluice-valve type is recommended. The combination of the advance detection method on cavitation surge oscillation and the sluice-valve type of obstacle plate becomes more effective against pump operation.
4) Even though the sluice-valve type of obstacle is inserted at low NPSH and partial flow rate, where cavitaion surge oscillation occurs, the insert does not sacrifice the improvement of cavitation performance of the pump by attachment of inducer because the inducer head is sufficiently high at partial flow rate to increase the inlet pressure of the main impeller.

Acknowledgments

Finally, authors should mention with their thanks that a part of this research was financially supported by the Grant-in-Aid from the Ministry of Education, Sports, Culture, Science and Technology (No. 17360081).

Nomenclature

A	Cross-section area of inducer inlet [m^2]	NPSH	Net positive suction head [m]
D	Tip blade diameter of inducer [m]	Q	Flow rate [m^3/s]
g	Gravitational acceleration [m^2/s]	U_t	Tip peripheral speed [m/s]
Δh	Increment of static head-rise on casing wall [m]	β_{1t}	Tip blade angle [deg]
H	Inducer head-rise [m]	τ	Dimensionless NPSH (= gH_{sv}/U_t^2)
H_{loss}	Flow loss due to installation of obstacle plate [m]	ϕ	Flow coefficient (= Q/AU_t)
H_{sv}	(= NPSH) [m]	ψ	Head-rise coefficient (= gH/U_t^2)
L	Distance between the obstacle plate and inducer inlet [m]	ψ_{loss}	Flow loss coefficient (= gH_{loss}/U_t^2)
m	Flow rate ratio normalized by shock-less flow rate	$\Delta\psi$	Increment of static head-rise coefficient on casing wall (= $g\Delta h/U_t^2$)
N	Rotational speed of inducer [min^{-1}]		

References

[1] Takamatsu, Y., Furukawa, A. and Ishizaka, K., 1984, "Method of Estimation of Required NPSH of Centrifugal Pump with Inducer," Proc. 1st China-Japan Joint Conference on Hydraulic Machinery and Equipment, pp. 253-261.

[2] Jacobsen, J. K., 1971, "Liquid Rocket Engine Turbo-pump Inducers," NASA SP-8052.

[3] Watanabe, T. and Kawata, 1978, "Y., Research on the Oscillations in Cavitating Inducer," IAHR Joint Symp. on Design and Operation of Fluid Machinery, pp. 265-274.

[4] Tsujimoto, Y., et al., 1997, "Observation of Oscillating Cavitation of an Inducer," Trans. ASME, J. Fluids Eng., Vol. 119, pp. 775-781.

[5] Yoshida, Y., Tsujimoto, Y., Kataoka, D., Horiguchi, H, and Wahl, F., 2001, "Effects of Leading Edge Cutback on Unsteady Cavitation in 4-Bladed Inducers," ASME J. Fluids Eng., Vol. 123, pp. 762-770.

[6] Kamijo, K., Yoshida, M. and Tsujimoto, Y., 1993, "Hydraulic and Mechanical Performance of LE-7 LOX Pump Inducer," AIAA Journal of Propulsion and Power, Vol. 9, pp. 819-826.

[7] Kurokawa, J., Imamura, H., Choi, Y.-D., Ito, M. and Kikuchi, M., 2005, "Suppression of Cavitation in Inducer by J-Grooves," (in Japanese), Turbomachinery(TSJ), 33-10, 592-600.

[8] Kim, J.-H., Ishizaka, K., et al., 2008, "Suppression Effect of Upstream Installed Ring-Shaped Obstacle Plate on Cavitation Surge in Pump Inducers," J. of Fluids Science and Technology, JSME, Vol. 3, No. 1, pp. 1-10.

[9] Furukawa, A., Ishizaka, K. and Watanabe, S., 2002, "Flow Measurement in Helical Inducer and Estimate of Fluctuating Blade Force in Cavitation Surge Phenomena," Japan Soc. Mech. Engrs. Inter. J., Ser.B, Vol. 45, pp. 672-677.

[10] Kim, J.-H., Atono T., Ishizaka, K., et al., 2008, "Rotating Behavior Observation of Cavitation in Inducer with Suction Axi-asymmetrical Plate," J. of Fluids Science and Technology, JSME, Vol. 3, No. 6, pp. 744-753.

[11] Ishizaka, K, and Furukawa, A., 1998, "Basic Study on Advance Detection of Cavitation Surge in Helical Inducer," Proc. US-Japan Seminar on Abnormal Flow Phenomena in Turbomachinery, Cavitation, 1-8.